ORIGINAL

Lipolysis-stimulated lipoprotein receptor is involved in fatty acid binding protein 4-mediated prostate cancer cell growth in bone

Tetsuyuki Takahashi[1], Takaaki Tsunematsu[2], and Hisanori Uehara[3]

[1]Department of Anatomy and Cell Biology, Faculty of Pharmacy, Research Institute of Pharmaceutical Sciences, Musashino University, Tokyo, Japan, [2]Department of Oral Molecular Pathology, Tokushima University Graduate School of Biomedical Sciences, Tokushima, Japan, [3]Division of Pathology, Tokushima University Hospital, Tokushima, Japan

Abstract : Obesity-induced excess adipokine production is associated with malignancy and mortality in prostate cancer. We previously showed that fatty acid binding protein 4 (FABP4), a major adipokine of mature adipocytes, promotes the progression of prostate cancer cell growth and invasion. In this report, we present lipolysis-stimulated lipoprotein receptor (LSR) as a newly identified binding partner for FABP4. Their binding induced Akt phosphorylation, whereas LSR knockdown (KD) failed to phosphorylate Akt. Intraosseous injection of LSR-KD prostate cancer cells showed smaller areas of intraosseous tumor, lower Ki-67 labeling indices, and lower numbers of phospho-Akt-positive cancer cells compared with control prostate cancer cells. Moreover, the contact co-culture of prostate cancer cells with bone marrow stromal cells (BMSCs) promoted FABP4 secretion by BMSCs. Our findings indicated that FABP4-mediated prostate cancer cell progression was regulated by cellular signaling via FABP4-LSR binding in the bone microenvironment. J. Med. Invest. 72 : 34-41, February, 2025

Keywords **:** *Lipolysis-stimulated lipoprotein receptor, fatty acid binding protein 4, prostate cancer, bone microenvironment*

INTRODUCTION

Obesity is associated with the tumor grade, mortality rate, and risk of prostate cancer (1-3). The number and size of adipocytes in patients with obesity are higher compared with individuals without obesity. Adipocytes secrete adipokines (adipocytokines), which exert various physiologic functions. Among them, leptin, interleukin-6, and tumor necrosis factor-α are overproduced in obese individuals and are positively associated with prostate cancer progression (4-7).

Fatty acid binding protein 4 (FABP4 ; A-FABP, aP2), a member of the FABP family, acts as a carrier of intracellular fatty acids. FABP4 is expressed in mature adipocytes and macrophages and is associated with rheumatoid arthritis, insulin resistance, type 2 diabetes mellitus, and atherosclerosis (8-11). Cancer cell-derived (endogenous) FABP4 acts as a tumor suppressor, whereas peripheral tissue- or blood-derived (exogenous) FABP4 exerts oncogenic effects (12-17). We previously demonstrated that treatment of prostate cancer cells with exogenous FABP4 promotes invasiveness and metastatic potential (18). These findings strongly suggest that an unknown mediator (probably the FABP4 receptor) on the cell surface transmits tumor-promoting signals. Here, we share the results of our investigations of this unknown mediator and present lipolysis-stimulated lipoprotein receptor (LSR) as a newly identified binding partner for FABP4.

Received for publication August 4, 2024 ; accepted October 9, 2024.

Address correspondence and reprint requests to Hisanori Uehara, MD, PhD, Division of Pathology, Tokushima University Hospital, 2-50-1 Kuramoto-cho, Tokushima, 770-8503, Japan and Fax : +81-88-633-9568. E-mail : uehara.h@tokushima-u.ac.jp

MATERIALS AND METHODS

Cells, animals, and reagents

DU145 human prostate cancer cells were obtained from RIKEN BioResource Center (Tsukuba, Japan) and maintained in RPMI 1640 medium supplemented with 10% FBS, 100 U/mL penicillin G, and 0.1 mg/mL streptomycin sulfate. Five-week-old male BALB/c and BALB/c nude mice (CLEA Japan, Tokyo, Japan) were maintained under specific pathogen-free conditions. All *in vivo* experiments were performed according to the Guideline for the Care and Use of Laboratory Animals of the University of Tokushima Graduate School and approved by the Animal Research Committee (approval number 11105). Recombinant human FABP4 (rFABP4), FITC-conjugated rFABP4, recombinant human LSR (rLSR) were obtained from ProSpec-Tany TechnoGene (Ness Ziona, Israel), Cayman Chemical (Ann Arbor, MI, USA), and United States Biological (Swampscott, MA, USA), respectively. The FABP4 inhibitor 2'-(5-Ethyl-3,4-diphenylpyrazol-1-yl)-biphenyl-3-yloxy was purchased from AstaTech (Bristol, PA, USA).

Identification of FABP4-binding protein in the membrane fraction

We isolated the membrane fraction from 1×10^7 DU145 cells using a Minute Plasma Membrane Protein Isolation and Cell Fractionation Kit (Invent Biotechnologies, Eden Prairie, MN, USA) and MPEX PTS Reagents for MS (GL Sciences, Tokyo, Japan) according to the manufacturer's protocol. The fraction was treated with or without rFABP4 (3 μg/sample) under rotation for 30 min at 37°C and then probed with 3 μg mouse monoclonal anti-FABP4 (Abnova, Taipei, Taiwan) under rotation for 3 h at 4°C. The resultant immunocomplexes were concentrated with Protein G-PLUS Agarose (Santa Cruz Biotechnology, Dallas, TX, USA) by rotating for 2 h at 4°C. FABP4-bound proteins were isolated by gradient SDS-PAGE (4%–20%), and the gels were stained using a Silver Stain MS Kit (Wako, Osaka, Japan). Augmented bands in FABP4-treated samples were cut out of the gel for analysis by nano-liquid chromatography–mass

spectrometry (nanoLC-MS/MS), and the results were used for protein identification using the Mascot Server software package (Matrix Science, Ueno, Tokyo). This analysis was contracted to the Support Center for Advanced Medical Sciences, Tokushima University Graduate School of Biomedical Sciences.

Flow cytometry

DU145 or LSR-knockdown (KD) DU145 cells (1×10^6) were probed with FITC-conjugated rFABP4 (0.3 or 1.0 μg) and incubated for 1 h at 37°C. For neutralization assays using rabbit polyclonal anti-LSR (Sigma-Aldrich, St. Louis, MO, USA), the cells were pretreated with anti-LSR (0.1, 0.3, or 1.0 μg) for 1 h at 37°C and then probed with FITC-conjugated rFABP4 (1.0 μg) and incubated for 1 h at 37°C. Flow cytometry analysis was performed using an EPICS XL Flow cytometer (Beckman Coulter, Brea, CA, USA) with an argon laser at 488 nm on samples containing 2×10^4 cells, and the mean fluorescence intensities (MFIs) were calculated.

Co-immunoprecipitation (Co-IP)

rFABP4 and rLSR (500 ng each) were mixed in RIPA buffer [19] and incubated for 30 min at 37°C. Then, the mixtures were probed with mouse or rabbit isotype IgG1 (1 : 100 ; R&D Systems, Minneapolis, MN, USA), mouse monoclonal anti-FABP4 (1 : 100), or rabbit polyclonal anti-LSR (1 : 100) and rotated for 3 h at 4°C. The resultant immunocomplexes were concentrated with Protein G-PLUS Agarose (Santa Cruz) by rotating for 2 h at 4°C, isolated by 15% or 10% SDS-PAGE, and subjected to immunoblotting.

LSR-KD

DU145 cells (3×10^5 cells/well) were seeded into six-well plates and preincubated overnight at 37°C. The following day, the cells were transfected with universal negative control siRNA #1 (Sigma-Aldrich) and LSR siRNA (SASI_Hs01_00187941 and SASI_Hs01_00348546 ; Sigma-Aldrich) using Lipofectamine RNAiMAX Transfection Reagent (Thermo Fisher Scientific, Carlsbad, CA, USA), according to the manufacturer's protocol. For *in vivo* experiments, we established stable LSR-KD cells using Non-target shRNA Control Transduction Particles (Sigma-Aldrich) or MISSION Lentiviral Transduction Particles for human LSR (TRCN0000020446, TRCN0000020448, TRCN0000274208, TRCN0000285149, and TRCN0000285151 ; Sigma-Aldrich) according to the manufacturer's protocol. The multiplicity of infection was set at 5 for all particles. After treating the infected cells with 2 μg/mL puromycin (Sigma-Aldrich) for 72 h, the viable cells were used to establish stable LSR-KD cells, and LSR protein expression was assessed by immunoblotting.

Immunoblotting

The Co-IP samples and untreated, treated, and LSR-KD cells were lysed for immunoblotting and protein level determination, as previously described [19]. The primary antibodies were rabbit monoclonal anti-FABP4 (1 : 2,000 ; Abcam, Cambridge, UK), rabbit polyclonal anti-LSR (1 : 1,000), rabbit polyclonal anti-phosphorylated Akt (1 : 500 ; Cell Signaling Technology, Danvers, MA, USA), rabbit polyclonal anti-Akt (1 : 1,000 ; Cell Signaling Technology), and rabbit polyclonal anti-actin (1 : 10,000 ; Sigma-Aldrich). The secondary antibodies were goat anti-rabbit IgG-HRP (1 : 100,000 ; Jackson ImmunoReseserch Laboratories, West Grove, PA, USA) and goat anti-mouse IgG-HRP (1 : 50,000 ; Thermo Fisher Scientific). An Immobilon Western Chemiluminescent HRP substrate (Millipore, Billerica, MA, USA) was used for signal detection.

Osteolytic bone metastasis model in nude mice

We examined the effects of control and stable LSR-KD DU145 cells using a previously described osteolytic bone metastasis model in nude mice [20]. FABP4 inhibitor was suspended in H_2O containing 4% Tween-80 and prepared at a concentration of 50 mg/kg. The mice received vehicle or FABP4 inhibitor by daily gavage for 8 weeks from the day after tumor cell transplantation. Then, they were sacrificed, the incidence of intraosseous tumor was recorded, and the tumor lesions underwent histological examination and IHC analysis.

Histological analyses

After fixation in 10% phosphate-buffered formaldehyde at room temperature for 48 h, the mouse hind limbs were decalcified in 10% EDTA (pH 7.4) for 12 days, embedded in paraffin, sectioned at 4–6 μm, and stained with hematoxylin and eosin (H&E). The area of the largest section of each tumor was measured using Nikon NIS-Elements D image analysis software (Nikon Instruments Inc., Melville, NY. USA). IHC was used to determine LSR, Ki-67, and cleaved caspase-3 expression. The primary antibodies were rabbit anti-LSR (1 : 100, Sigma-Aldrich), mouse monoclonal anti-Ki-67 (1 : 50, DakoCytomation, Glostrup, Denmark), and rabbit polyclonal anti-phospho-Akt (1 : 300, Cell Signaling Technology). The Ki-67 labeling index was calculated as the percentage of Ki-67-positive cells in >500 cells for each tumor. The number of phospho-Akt-positive cells was counted in 10 fields (0.6 mm^2/field), excluding necrotic areas, using Olympus BX51 microscope (Olympus, Tokyo, Japan) and DS-Ri1 digital camera (Nikon).

Bone marrow stromal cells (BMSCs) isolation

Bone marrow was collected from euthanized five-week-old male BALB/c mice by flushing femurs and tibias with DMEM supplemented with 10% FBS. The cells were washed twice in serum-free DMEM and then cultured in a 100-mm culture dish at 37°C. After 3 days, nonadherent cells were removed by two to three washes with PBS, and adherent cells were cultured in DMEM supplemented with 10% FBS for 4 days before experimental use.

Coculture assay

DU145 cells and BMSCs underwent contact and bilayer coculture. For the contact coculture, DU145 cells and BMSCs were mixed at a ratio of 1 : 1 (4×10^5 cells each). For the bilayer coculture, BMSCs were seeded into a six-well plate (4×10^5 cells/well). Then, a cell culture insert (PET membrane, 0.4 μm pore size ; Falcon, Franklin Lakes, NJ, USA) was placed on the top of each wells, onto which equal numbers of DU145 cells were seeded. After incubation for 72 h at 37°C, the culture supernatants were withdrawn, and FABP4 levels were measured using an adipocyte FABP (FABP4) Human ELISA Kit (BioVendor, Brno, Czech Republic).

Statistical analysis

A two-tailed Student's t-test was employed for statistical analyses of the data. *P*-values < 0.05 were considered statistically significant.

RESULTS

FABP4 interacts with LSR

To identify novel binding partners for FABP4, we tested the membrane fractions from DU145 cells with rFABP4 followed by immunoprecipitation with anti-FABP4. SDS-PAGE and

subsequent silver staining revealed an augmented band in the FABP4-treated group, which extracted for nanoLC-MS/MS analysis. The results revealed that LSR, which localizes on the plasma membrane and is a cell surface receptor, was a candidate binding partner. The Mascot search showed extracellular and intracellular LSR protein regions as hits for FABP4-bound peptide fragments (Fig. 1A). Next, we investigated whether FABP4 actually binds to the cell surface, and this was confirmed by a dose-dependent increase in FITC-conjugated rFABP4-induced MFI (Fig. 1B), while pretreatment with anti-LSR showed dose-dependent inhibition of the same. Furthermore, Co-IP also revealed that rFABP4 interact with rLSR (Fig. 1C and 1D).

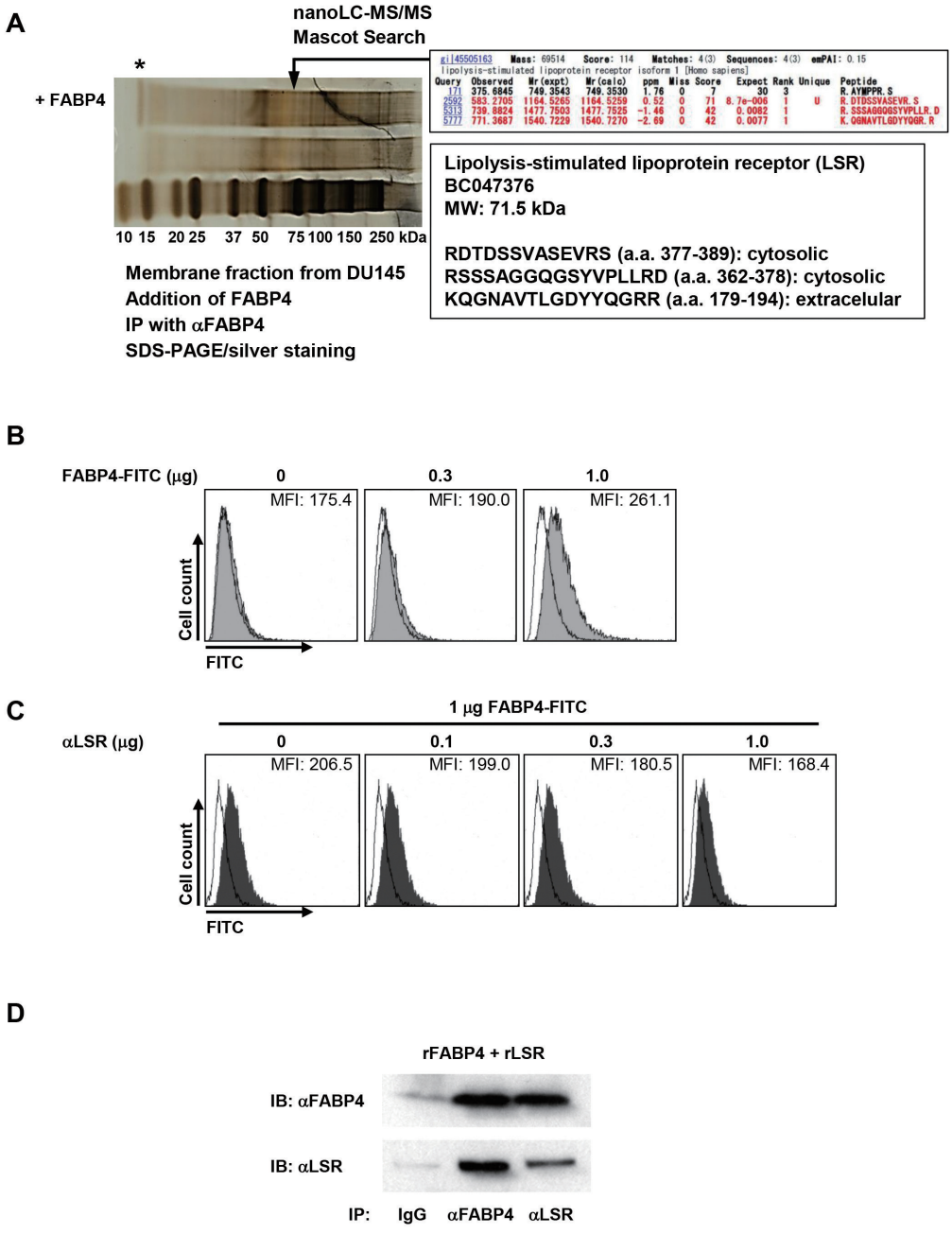

Figure 1. Identification of LSR as a binding partner for FABP4.
(A) Following anti-FABP4 immunoprecipitation of the membrane fraction of DU145 cells treated with or without rFABP4, each immunoprecipitant underwent SDS-PAGE and silver staining (left). Augmented bands in FABP4-treated samples were cut out of the gel for nanoLC-MS/MS analysis, and a Mascot search was performed (right). Raw data and detailed information for LSR are shown. *, added rFABP4-derived band. (B) Flow cytometry analysis results of DU145 cells treated with 0.3 or 1.0 μg FITC-conjugated rFABP4. The MFI of each group was used as an indicator of binding between FITC-conjugated rFABP4 and the cell surface. Open histograms represent profiles of non-treatment group. (C) Flow cytometry analysis results of DU145 cells pretreated with 0.1, 0.3, or 1.0 μg anti-LSR antibody prior to FITC-conjugated rFABP4 treatment (1.0 μg). The MFI of each group was used as an indicator of binding between FITC-conjugated rFABP4 and the cell surface. Open histograms represent profiles of non-treatment group. (D) rFABP4 and rLSR were mixed, co-immunoprecipitated with isotype IgG, anti-FABP4 antibody, and anti-LSR antibody and subjected to immunoblotting using anti-FABP4 and anti-LSR antibodies. *IB*, immunoblotting ; *IP*, immunoprecipitation.

Interaction of FABP4 with LSR promotes Akt activation

A KD experiment to clarify whether FABP4 was a binding partner for LSR revealed that LSR-KD using siRNA #7941 successfully decreased LSR expression and inhibited FITC-conjugated rFABP4-induced MFI increases (Fig. 2A and 2B). Furthermore, LSR-KD using siRNA #7941 markedly decreased Akt phosphorylation by FABP4 (Fig. 2C).

LSR regulates intraosseous prostate cancer cell growth

Because DU145 cells cause osteolytic lesions when transplanted into bone, we used an osteolytic bone metastasis model (21) to assess the effect of LSR on intraosseous tumor growth. We established LSR-KD DU145 cells using lentiviral particles. Of the five viral clones examined, the clone with TRCN0000274208-mediated KD was the most effective (Fig. 3A). Therefore, we injected TRCN0000274208-infected DU145 cells into the tibial tuberosity. IHC revealed that LSR downregulation was successfully sustained until the end of the experiment. Additionally, administration of FABP4 inhibitor, which inhibits the binding between FABP4 and fatty acids, did not influence LSR expression (Fig. 3B). Regardless of the presence of FABP4 inhibitor, the incidence of intraosseous tumor lesions was decreased by LSR-KD (Fig. 3B). LSR-KD with FABP4 inhibitor also showed significantly decreased mean tumor areas. Additionally, LSR-KD significantly decreased Ki-67 labeling indices in intraosseous tumor lesions and FABP4 inhibitor administration further decreased the Ki-67 labeling index in LSR-KD cells (Fig. 3C and 3D). IHC for phospho-Akt revealed that LSR-KD significantly decreased the number of phospho-Akt-positive cells in tumor lesions, but the FABP4 inhibitor did not enhance this effect (Fig. 3E).

The tumor microenvironment regulates intraosseous FABP4 level

A coculture assay was performed to determine whether cells adjacent to cancer cells in the bone microenvironment were a source of exogenous FABP4. An experimental schema was illustrated in Fig. 4A. A single culture of BMSCs secreted FABP4, whereas that of DU145 did not. Bilayer coculture of BMSCs with DU145 slightly increased FABP4 secretion in BMSCs, while mixed coculture, which mimics cell–cell contact conditions, significantly increased FABP4 secretion in BMSCs (Fig. 4B).

DISCUSSION

LSR is involved in forming tight junctions of epithelial cells together with components such as tricellulin, apoptosis-stimulating protein of p53-2, claudins, occludins, and Hippo/YAP (22). LSR-KD increases the malignancy of bladder, colon, and pancreatic cancer cells (23-25), whereas LSR promotes malignancy in breast and ovarian cancer cells (26, 27), suggesting the bidirectional function of LSR in cancer cell progression. The effect of LSR on prostate cancer cell progression has yet to be reported, although its expression has been confirmed in hormone-resistant cell line PC-3 (28). However, we found that LSR-KD in DU145 cells inhibited exogenous FABP4-induced Akt activation (18), indicating that LSR positively regulates prostate cancer cell progression. Additionally, both extracellular and intracellular

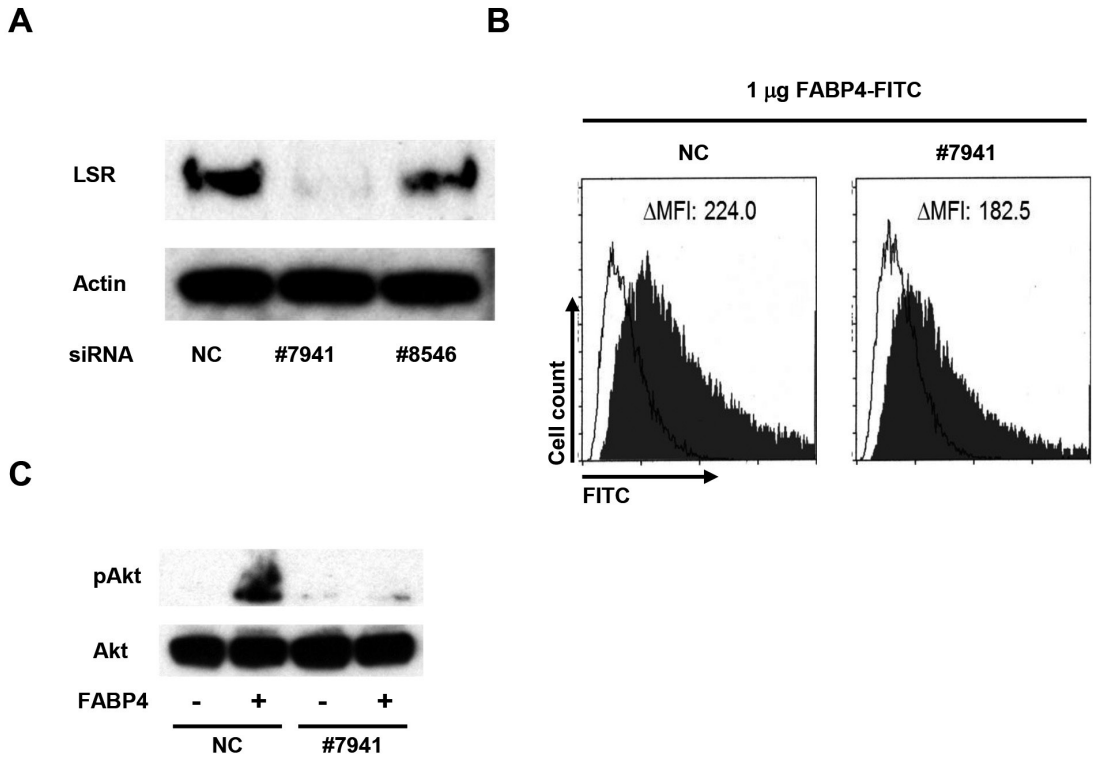

Figure 2. Interaction of FABP4 with LSR promotes Akt activation.
(A) DU145 cells were transfected with two types of LSR siRNA (#7941 and #8546), and the LSR protein levels were determined using immunoblotting. Actin was used as an internal control. *NC*, universal negative control siRNA #1. (B) Flow cytometry results of control and LSR-KD DU145 cells treated with 1.0 μg FITC-conjugated rFABP4. Increased levels of MFI were used as indicators of the effect of LSR-KD. Open histograms represent profiles of non-treatment group. (C) Immunoblot results of control and LSR-KD DU145 cells treated with 1.0 μg rFABP4 for 24 h to determine the effect on phosphorylated Akt (pAkt).

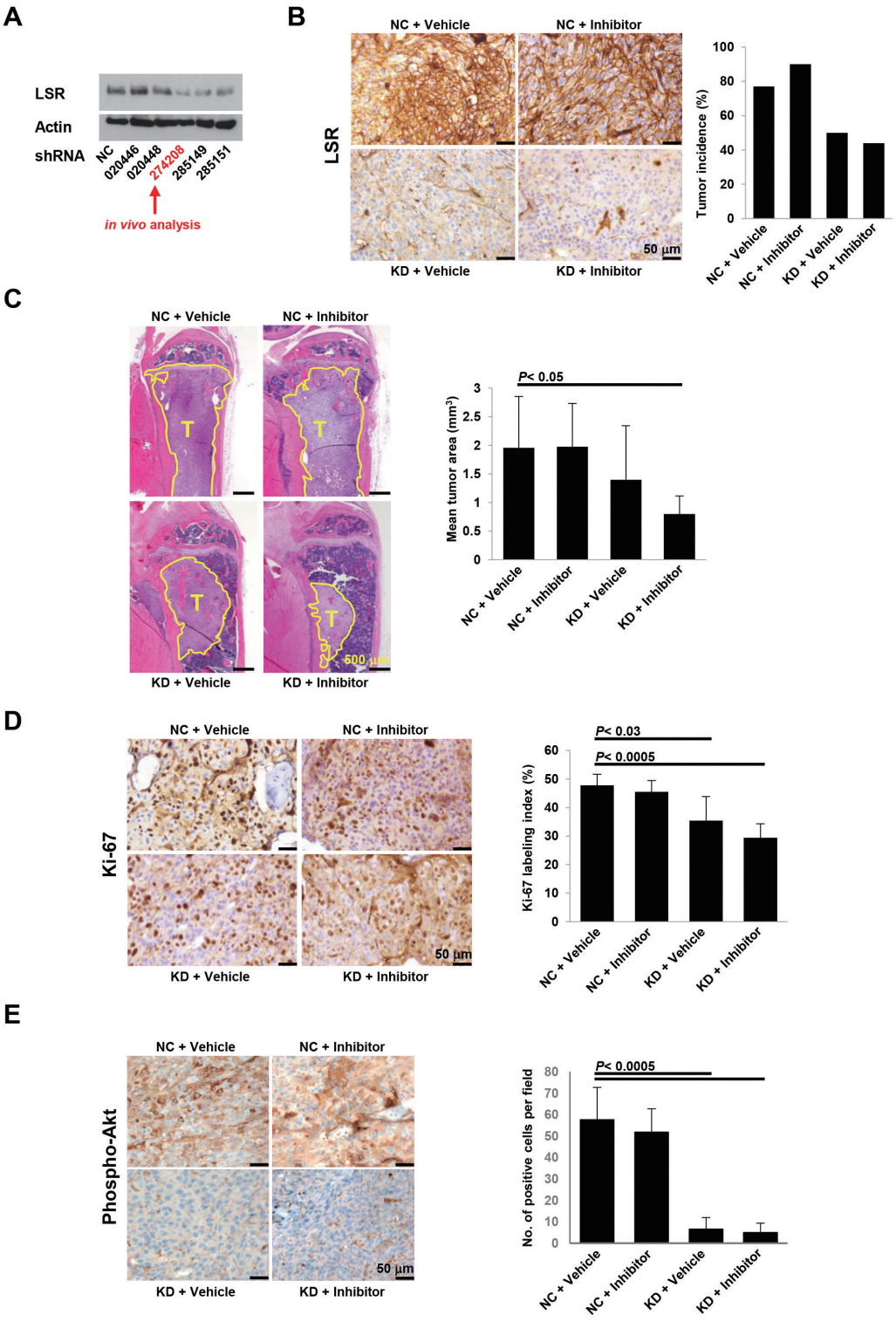

Figure 3. Effect of LSR-KD and FABP4 inhibitor on prostate cancer bone metastasis and prostate cancer growth in bone.
(A) DU145 cells were infected with five types of shRNA lentiviral particles for LSR, and then the LSR protein levels were determined using immunoblotting. Actin was used as an internal control. *NC*, Non-target shRNA Control Transduction Particles. (B) Representative images of IHC for LSR in the intraosseous tumor lesions (left). Mice were injected with FABP4 inhibitor-treated or -untreated control and LSR-KD DU145 cells. The tumor incidence was calculated for each treatment group (n = 9-10/group) (right). *Scale bar*, 50 μm. (C) H&E results for tumor sizes in the intraosseous tumor lesions (left) and mean tumor areas (n = 9-10/group) for each group (right). Error bars represent the SD. *P*-values < 0.05 were considered statistically significant. *Scale bar*, 500 μm. (D) IHC results for Ki-67 in the intraosseous tumor lesions (left) and Ki-67 labeling indices (n = 9-10/group) for each group (right). Error bars represent the SD. *P*-values < 0.05 were considered statistically significant. *Scale bar*, 50 μm. (E) IHC results for phospho-Akt in the intraosseous tumor lesions (left) and the number of phospho-Akt-positive cells per field (n = 9–10) for each group (right). Error bars represent the SD. *P*-values < 0.05 were considered statistically significant. *Scale bar*, 50 μm.

peptide fragments of LSR were identified as binding partners for FABP4, suggesting two distinct binding patterns : (1) typical binding at an extracellular region, as with a ligand and receptor, and (2) a unique process of intracellular binding following FABP4 internalization into the cytosol. Various growth factor receptors, including epidermal growth factor receptor and insulin receptor, have been reported to be internalized after binding with their ligand (29, 30). It has also been reported that the *Clostridium perfringens* iota-toxins binds to LSR and mediates the entry of LSR into the cytoplasm (31). At the very least, we showed that exogenous FABP4 binds to extracellular LSR (Fig. 1B and 1C). Further investigation to confirm the interaction of FABP4 with the intracellular region of LSR and the internalization of LSR by FABP4 treatment is necessary. LSR-KD decreased exogenous FABP4-induced Akt activation, strongly suggesting that FABP4-LSR binding activates the PI3K/Akt pathway, which is inhibited by neutralizing antibodies against LSR (32), and that FABP4 is the main activation component of LSR-mediated PI3K/Akt signaling.

The bone microenvironment also affects the progression of bone metastasis in prostate cancer. Osteoclast, osteoblast, BMSCs, and immune cells participate in cancer cell-mediated bone recycling disorder and tumor progression (33-35). The association between LSR expression and the behavior of prostate tumors in bone remains unknown. The injection of control or LSR-KD DU145 cells into mouse bone revealed that LSR-KD reduced tumor growth, decreased the Ki-67 labeling index, and decreased Akt activation, indicating the association of LSR with prostate cancer cell progression in bone. Coculture experiments using DU145 cells and BMSCs showed significant increases in FABP4 secretion in BMSCs in a mixed coculture, strongly suggesting that physical contact between prostate cancer cells and BMSCs triggers exogenous FABP4 supplementation in bone metastatic lesions. Exogenous FABP4 binds to LSR and induces Akt activation, and we previously reported that physical contact between prostate cancer cells and osteoblasts enhanced FABP4 expression (36). Therefore, the BMSC- and osteoblast-associated FABP4-LSR-PI3K/Akt axis may accelerate for prostate cancer progression in bone (Fig. 5). FABP4 inhibitor enhanced the effect of LSR-KD on intraosseous tumor growth and the Ki-67 labeling index, suggesting that the fatty acid-binding status of FABP4 alters the effect of exogenous FABP4 on LSR-mediated cellular

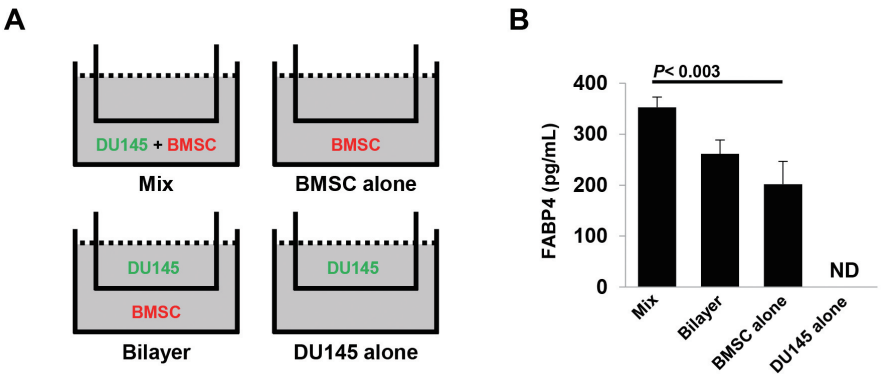

Figure 4. Contact coculture of DU145 cells with BMSCs augments FABP4 secretion from BMSCs. (A) An experimental schema of coculture. Mixed and bilayer coculture of DU145 cells with BMSCs and monocultures of DU145 and BMSCs, respectively, were performed. (B) The mean levels of secreted FABP4 in the culture supernatants ($n = 3$/group) were determined by ELISA (right). Error bars represent the SD. *ND*, not detected. *P*-values < 0.05 were considered statistically significant.

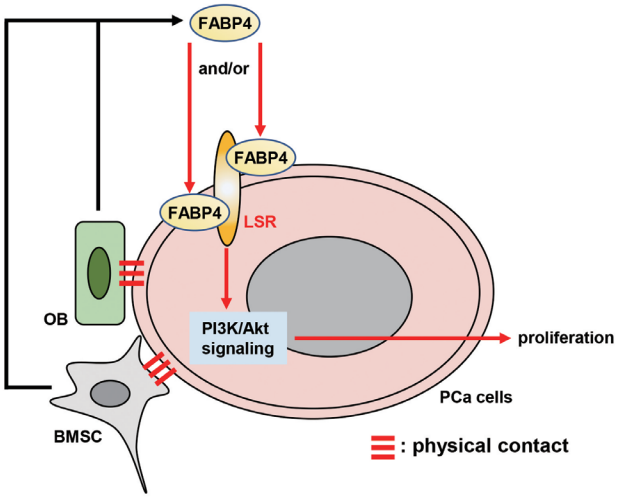

Figure 5. Schematic representation of the mechanism of the BMSC- and osteoblast-associated FABP4-LSR-PI3K/Akt axis in prostate cancer cells. This illustration is based on the results of this study and our previous report (36).

signaling in prostate cancer cells.

Monoclonal antibodies for LSR exert therapeutic activity against endometrial and ovarian cancer (37, 38), and our findings indicate that this could also be effective for prostate cancer bone metastasis. Although the effectiveness of interference with cell-cell interactions (prostate cancer cells with BMSCs or osteoblasts) and the antagonistic effect of anti-FABP4 for prostate cancer bone metastasis have yet to be assessed, these methodologies may have therapeutic potential for prostate cancer bone metastasis. Thus, additional investigations of their antimetastatic potential are warranted.

CONFLICT OF INTEREST

The authors declare that they have no known competing financial interests or personal relationships that could have influenced the work reported in this paper.

ACKNOWLEDGEMENT

This study was supported by JSPS KAKENHI (JP15K08403 and JP21K06538), awarded to H. Uehara and T. Takahashi, respectively.

REFERENCES

1. Fowke JH, Motley SS, Concepcion RS, Penson DF, Barocas DA : Obesity, body composition, and prostate cancer. BMC Cancer 12 : 23, 2012
2. Rundle A, Jankowski M, Kryvenko ON, Tang D, Rybicki BA : Obesity and future prostate cancer risk among men after an initial benign biopsy of the prostate. Cancer Epidemiol Biomarkers Prev 22 : 898-904, 2013
3. Rivera-Izquierdo M, Pérez de Rojas J, Martínez-Ruiz V, Pérez-Gómez B, Sánchez MJ, Khan KS, Jiménez-Moleón JJ : Obesity as a risk factor for prostate cancer mortality : A systematic review and dose-response meta-analysis of 280,199 patients. Cancers 13 : 4169, 2021
4. Onuma M, Bub JD, Rummel TL, Iwamoto Y : Prostate cancer cell-adipocyte interaction : leptin mediates androgen-independent prostate cancer cell proliferation through c-Jun NH2-terminal kinase. J Biol Chem 278 : 42660-42667, 2003
5. Okamoto M, Lee C, Oyasu R : Interleukin-6 as a paracrine and autocrine growth factor in human prostatic carcinoma cells in vitro. Cancer Res 57 : 141-146, 1997
6. Bennett JL, Jackson BN, Miller RJ, Tsui H, Mertin-Caraballo M : IL-6 evoked biochemical changes in prostate cancer cells. Cytokine 161 : 156079, 2023
7. Wang X, Yang L, Huang F, Zhang Q, Liu S, Ma L, You Z : Inflammatory cytokines IL-17 and TNF-α upregulate PD-L1 expression in human prostate and colon cancer cells. Immunol Lett 184 : 7-14, 2017
8. Cerezo LA, Kuklová M, Hukejová H, Vernerová Z, Pešáková V, Pecha O, Veigl D, Haluzík M, Pavelka K, Vencovskŷ J, Senolt L : The level of fatty acid-binding protein 4, a novel adipokine, is increased in rheumatoid arthritis and correlates with serum cholesterol levels. Cytokine 64 : 441-447, 2013
9. Hotamisligil GS, Johnson RS, Distel RJ, Ellis R, Papaioannou VE, Spiegelman BM : Uncoupling of obesity from insulin resistance through a targeted mutation in aP2, the adipocyte fatty acid binding protein. Science 274 : 1377-1379, 1996
10. Djoussé L, Gaziano JM : Plasma levels of FABP4, but not FABP3, are associated with increased risk of diabetes. Lipids 47 : 757-762, 2012
11. Gormez S, Erdim R, Akan G, Caynak B, Duran C, Gunay D, Sozer V, Atalar F : Relationships between visceral/subcutaneous adipose tissue FABP4 expression and coronary atherosclerosis in patients with metabolic syndrome. Cardiovasc Pathol 46 : 107192, 2020
12. De Santis ML, Hammamieh R, Das R, Jett M : Adipocyte-fatty acid binding protein induces apoptosis in DU145 prostate cancer cells. J Exp Ther Oncol 4 : 91-100, 2004
13. Harjes U, Bridges E, Gharpure KM, Roxanis I, Sheldon H, Miranda F, Mangala LS, Pradeep S, Lopez-Berestein G, Ahmed A, Fielding B, Sood AK, Harris AL : Antiangiogenic and tumor inhibitory effects of downregulating tumour endothelial FABP4. Oncogene 36 : 912-921, 2017
14. Wu Z, Jeong JH, Ren C, Yang L, Ding L, Li F, Jiang D, Zhu Y, Lu J : Fatty acid-binding protein 4 (FABP4) suppresses proliferation and migration of endometrial cancer cells via PI3K/Akt pathway. Onco Targets Ther 14 : 3929-3942, 2021
15. Nieman KM, Kenny HA, Penicka CV, Ladanyi A, Buell-Gutbrod R, Zillhardt MR, Romero IL, Carey MS, Mills GB, Hotamisligil GS, Yamada SD, Peter ME, Gwin K, Lengyel E : Adipocytes promote ovarian cancer metastasis and provide energy for rapid tumor growth. Nat Med 17 : 1498-1503, 2011
16. Mukherjee A, Chiang CY, Daifotis HA, Nieman KM, Fahrmann JF, Lastra RR, Romero I, Fiehn O, Lengyel E : Adipocyte-induced FABP4 expression in ovarian cancer cells promotes metastasis and mediates carboplatin resistance. Cancer Res 80 : 1748-1761, 2020
17. Yang J, Liu S, Li Y, Fan Z, Meng Y, Zhou B, Zhang G, Zhan H : FABP4 in macrophages facilitates obesity-associated pancreatic cancer progression via NLRP3/IL-1β axis. Cancer Lett 575 : 216403, 2023
18. Uehara H, Takahashi T, Oha M, Ogawa H, Izumi K : Exogenous fatty acid binding protein 4 promotes human prostate cancer cell progression. Int J Cancer 135 : 2558-2568, 2014
19. Takahashi T, Uehara H, Bando Y, Izumi K : Soluble EP2 neutralizes prostaglandin E2-induced cell signaling and inhibits osteolytic tumor growth. Mol Cancer Ther 7 : 2807-2816, 2008
20. Uehara H, Kim SJ, Karashima T, Shepherd DL, Fan D, Tsan R, Killion JJ, Logothetis C, Mathew P, Fidler IJ : Effects of blocking platelet-derived growth factor-receptor signaling in a mouse model of experimental prostate cancer bone metastasis. J Natl Cancer Inst 95 : 458-470, 2003
21. Nemeth JA, Harb JF, Barroso Jr U, He Z, Grignon DJ, Cher ML : Severe combined immunodeficient-hu model of human prostate cancer metastasis to human bone. Cancer Res 59 : 1987-1993, 1999
22. himada H, Kohno T, Konno T, Okada T, Saito K, Shindo Y, Kikuchi S, Tsujiwaki M, Ogawa M, Matsuura M, Saito T, Kojima T : The roles of tricellular tight junction protein Angulin-1/Lipolysis-stimulated lipoprotein receptor (LSR) in endometriosis and endometrioid-endometrial carcinoma. Cancers 13 : 6341, 2021
23. Herbsleb M, Birkenkamp-Demtroder K, Thykjaer T, Wiuf C, Hein AMK, Orntoft TF, Dyrskjøt L : Increased cell motility and invasion upon knockdown of lipolysis stimulated lipoprotein receptor (LSR) in SW780 bladder cancer cells. BMC Med Genomics 1 : 31, 2008
24. Czulkies BA, Mastroianni J, Lutz L, Lang S, Schwan C, Schmidt G, Lassmann S, Zeiser R, Aktories K, Papatheodorou P : Loss of LSR affects epithelial barrier

integrity and tumor xenograft growth of CaCo-2 cells. Oncotarget 8 : 37009-37022, 2017
25. Kyuno T, Kyuno D, Kohno T, Konno T, Kikuchi S, Arimoto C, Yamaguchi H, Imamura M, Kimura Y, Kondoh M, Takemasa I, Kojima T : Tricellular tight junction protein LSR/angulin-1 contributes to the epithelial barrier and malignancy in human pancreatic cancer cell line. Histochem Cell Biol 153 : 5-16, 2020
26. Reaves DK, Fagan-Solis KD, Dunphy K, Oliver SD, Scott DW, Fleming JM : The role of lipolysis stimulated lipoprotein receptor in breast cancer and directing breast cancer cell behavior. PLos One 9 : e91747, 2014
27. Takahashi Y, Serada S, Ohkawara T, Fujimoto M, Hiramatsu K, Ueda Y, Kimura T, Takemori H, Naka T : LSR promotes epithelial ovarian cancer cell survival under energy stress through the LKB1-AMPK pathway. Biochem Biophys Res Commun 537 : 93-99, 2021
28. Parsana P, Amend SR, Hernandez J, Pienta KJ, Battle A : Identifying global expression patterns and key regulators in epithelial to mesenchymal transition through multistudy integration. BMC Cancer 17 : 447, 2017
29. Schlessinger J : Allosteric regulation of the epidermal growth factor receptor kinase. J Cell Biol 103 : 2067-2072, 1986
30. Goh LK, Sorkin A : Endocytosis of receptor tyrosine kinases. Cold Spring Harb Perspect Biol 5 : a017459, 2013
31. Nagahama M, Takehara M, Seike S, Sakaguchi Y : Cellular uptake and cytotoxicity of *Clostridium perfringens* Iota-toxin. Toxins 15 : 695, 2023
32. Sugase T, Takahashi T, Serada S, Fujimoto M, Ohkawara T, Hiramatsu K, Koh M, Saito Y, Tanaka K, Miyazaki Y, Makino T, Kurokawa Y, Yamasaki M, Nakajima K, Hanazaki K, Mori M, Doki Y, Naka T : Lipolysis-stimulated lipoprotein receptor overexpression is a novel predictor of poor clinical prognosis and a potential therapeutic target in gastric cancer. Oncotarget 9 : 32917-32928, 2018
33. Esposito M, Guise T, Kang Y : The biology of bone metastasis. Cold Spring Harb Perspect Med 8 : a031252, 2018
34. Hensel J, Wetterwald A, Temanni R, Keller I, Riether C, van der Pluijm G, Cecchini MG, Thalmann GN : Osteolytic cancer cells induce vascular/axon guidance processes in the bone/bone marrow stroma. Oncotarget 9 : 28877-28896, 2018
35. Arellano DL, Juárez P, Verdugo-Meza A, Almeida-Luna PS, Corral-Avila JA, Drescher F, Olvera F, Jimenéz S, Elzey BD, Guise TA, Fournier PGJ : Bone microenvironment-suppressed T cells increase osteoclast formation and osteolytic bone metastasis in mice. J Bone Miner Res 37 : 1446-1463, 2022
36. Shiirevnyamba A, Takahashi T, Shan H, Ogawa H, Yano S, Kanayama H, Izumi K, Uehara H : Enhancement of osteoclastogenic activity in osteolytic prostate cancer cells by physical contact with osteoblasts. Br J Cancer 104 : 505-513, 2011
37. Nagase Y, Hiramatsu K, Funauchi M, Shiomi M, Masuda T, Kakuda M, Nakagawa S, Miyoshi A, Matsuzaki S, Kobayashi E, Kimura T, Serada S, Ueda Y, Naka T, Kimura T : Anti-lipolysis-stimulated lipoprotein receptor monoclonal antibody as a novel therapeutic agent for endometrial cancer. BMC Cancer 22 : 679, 2022
38. Kanda M, Serada S, Hiramatsu K, Funauchi M, Obata K, Nakagawa S, Ohkawara T, Murata O, Fujimoto M, Chiwaki F, Sasaki H, Ueda Y, Kimura T, Naka T : Lipolysis-stimulated lipoprotein receptor-targeted antibody-drug conjugate demonstrates potent antitumor activity against epithelial ovarian cancer. Neoplasia 35 : 100853, 2023